

# Soliton pulse compression in photonic band-gap fibers.

Dimitre G. Ouzounov, Christopher J. Hensley and Alexander L. Gaeta

*School of Applied and Engineering Physics, Cornell University, Ithaca, NY 14853*

[dimitre.ouzounov@cornell.edu](mailto:dimitre.ouzounov@cornell.edu), [a.gaeta@cornell.edu](mailto:a.gaeta@cornell.edu)

Natesan Venkateraman, Michael T. Gallagher and Karl W. Koch

*Corning Inc, Corning, NY 14831*

**Abstract:** We report on pulse compression using a hollow-core photonic band-gap fiber filled with Xe. Output pulses with megawatt peak powers and durations of 50 fs have been generated from 120-fs input pulses. The large third-order dispersion inherent in these fibers degrades the optimal compression ratio and prevents generation of even shorter pulses. Nevertheless, for picosecond input pulses, compression to less than 100 fs is predicted.

© 2005 Optical Society of America

**OCIS codes:** (060.4370) Nonlinear optics, fibers; (060.5530) Pulse propagation and solitons; (190.7110) Ultrafast nonlinear optics; (320.5520) Pulse compression

---

## References and links

1. R. F. Cregan, B. J. Mangan, J. C. Knight, T. A. Birks, P. St. J. Russell, P. J. Roberts, and D. A. Allan, "Single-mode photonic band gap guidance of light in air," *Science* **285**, 1537–1539 (1999).
2. C. M. Smith, N. Venkateraman, M. T. Gallagher, D. Muller, J. A. West, N. F. Borrelli, D. C. Allan, and K. W. Koch, "Low-loss hollow-core silica/air photonic bandgap fibre," *Nature* **424**, 657–659 (2003).
3. B. J. Mangan, L. Farr, A. Langford, P. J. Roberts, D. P. Williams, F. Couny, M. Lawman, M. Mason, S. Coupland, R. Flea, H. Sabert, T. A. Birks, J. C. Knight, P. St. J. Russell, "Low loss (1.7 dB/km) hollow core photonic bandgap fiber," postdeadline paper PDP24, OFC'04 (Los Angeles, 2004).
4. D. G. Ouzounov, F. R. Ahmad, D. Muller, N. Venkateraman, M. T. Gallagher, M. G. Thomas, J. Silcox, K. W. Koch, and A. L. Gaeta, "Generation of megawatt optical solitons in hollow-core photonic band-gap fibers," *Science* **301**, 1702–1704 (2003).
5. D. G. Ouzounov, C. J. Hensley, A. L. Gaeta, N. Venkateraman, M. T. Gallagher, and K. W. Koch, "The effective nonlinearity of hollow-core photonic band-gap fibers," in preparation.
6. F. Luan, J. C. Knight, P. St. J. Russell, S. Campbell, D. Xiao, D. T. Reid, B. J. Mangan, D. P. Williams, and P. J. Roberts, "Femtosecond soliton pulse delivery at 800 nm wavelength in hollow-core photonic bandgap fibers," *Opt. Express* **12**, 835–840 (2004).  
<http://www.opticsexpress.org/abstract.cfm?URI=OPEX-12-5-835>
7. G. Humbert, J. C. Knight, G. Bouwmans, P. St. J. Russell, D. P. Williams, P. J. Roberts, B. J. Mangan, "Hollow core photonic crystal fibers for beam delivery," *Opt. Express* **12**, 1477–1484 (2004).  
<http://www.opticsexpress.org/abstract.cfm?URI=OPEX-12-8-1477>
8. F. Benabid, J. C. Knight, G. Antonopoulos, P. St. J. Russell, "Stimulated Raman scattering in hydrogen-filled hollow-core photonic crystal fiber," *Science* **298** 399–402 (2002)
9. F. Benabid, G. Bouwmans, J. C. Knight, P. St. J. Russell, and F. Couny, "Ultrahigh efficiency laser wavelength conversion in a gas-filled hollow core photonic crystal fiber by pure stimulated rotational raman scattering in molecular hydrogen," *Phys. Rev. Lett.* **93** 123903 (2004)
10. S. O. Konorov, A. B. Fedotov, and A. M. Zheltikov, "Enhanced four-wave mixing in a hollow-core photonic-crystal fiber," *Opt. Lett.* **28** 1448 (2003).
11. S. Ghosh, J. E. Sharping, D. G. Ouzounov and A. L. Gaeta, "Coherent resonant interactions and slow light with molecules confined in photonic band-gap fiber," *Phys. Rev. Lett.* **94**, 093902 (2005).

12. S. O. Konorov, A. M. Zheltikov, P. Zhou, A. P. Tarasevitch, and D. von der Linde, "Self-channeling of subgigawatt femtosecond laser pulses in a ground-state waveguide induced in the hollow core of a photonic crystal fiber," *Opt. Lett.* **29**, 1521 (2004).
13. G. P. Agrawal, *Nonlinear Fiber Optics* (Academic Press, San Diego, ed. 3, 2001).
14. L. F. Mollenauer, R. H. Stolen, J. P. Gordon, and W. J. Tomlinson, "Extreme picosecond pulse narrowing by means of soliton effect in single-mode optical fibers," *Opt. Lett.* **8**, 289–291 (1983).
15. G. P. Agrawal, "Effect of intrapulse stimulated Raman scattering on soliton-effect pulse compression in optical fibers," *Opt. Lett.* **15**, 224–226 (1990).
16. K. C. Chan and H. F. Liu, "Effect of third-order dispersion on soliton-effect pulse compression," *Opt. Lett.* **19**, 49–51 (1994).
17. K. C. Chan and H. F. Liu, "Short Pulse Generation by Higher Order Soliton-Effect Compression: Effects of Optical Fiber Characteristics," *IEEE J. Quantum Electron.* **31**, 2226–2235 (1995).
18. P. Beaud, W. Hodel, B. Zysset, and H. P. Weber, "Ultrashort pulse propagation, pulse breakup, and fundamental soliton formation in a single-mode optical fiber," *IEEE J. Quantum Electron.* **23**, 1938–1946 (1987).
19. K. Chan and W. Cao, "Improved soliton-effect pulse compression by combined action of negative third-order dispersion and Raman self-scattering in optical fibers," *J. Opt. Soc. Am. B* **15**, 2371–2375 (1998).
20. G. P. Agrawal, *Applications of Nonlinear Fiber Optics* (Academic Press, San Diego, 2001).
21. M. Nisoli, S. De Silvestri, and O. Svelto, "Generation of high energy 10 fs pulses by a new pulse compression technique," *Appl. Phys. Lett.* **68**, 2793–2795 (1996).
22. T. Sudmeyer, F. Brunner, E. Innerhofer, R. Paschotta, K. Furusawa, J. C. Baggett, T. M. Monro, D. J. Richardson, and U. Keller, "Nonlinear femtosecond pulse compression at high average power levels by use of a large-mode-area holey fiber," *Opt. Lett.* **28**, 1951–1953 (2003).
23. T. Brabec and F. Krausz, "Nonlinear optical pulse propagation in the single-cycle regime," *Phys. Rev. Lett.* **78**, 3283 (1997).
24. E. T. J. Nibbering, G. Grillon, M. A. Franco, B. S. Prade, and A. Mysyrowicz, "Determination of the inertial contribution to the nonlinear refractive index of air,  $N_2$ , and  $O_2$  by use of unfocused high-intensity femtosecond laser pulses," *J. Opt. Soc. Am. B* **14**, 650–660 (1997).

## 1. Introduction

Photonic band-gap fibers (PBGFs) have attracted significant interest since their first realization [1] and have started to find their way into applications once low-loss versions were developed [2, 3]. A photonic band gap is formed by the the two-dimensional structured cladding, which enables guiding in a low refractive index region (air, vacuum). This can lead to a reduction in the total fiber nonlinearity by more than 1000 times as compared with conventional silica-core step-index fiber [4, 5]. Waveguide dispersion dominates the total dispersion and is anomalous over most of the transmission window [4], which in combination with the low nonlinearity allows for the generation of megawatt optical solitons [4, 6]. As a result of the much smaller nonlinearity and larger damage threshold as compared with conventional fibers, PBGFs emerge as a viable alternative for high-energy pulse delivery [7]. By filling the fiber core with gases other than air, PBGFs could find applications in nonlinear and quantum optics of molecular and atomic gases since extremely long interaction lengths can be achieved. Non-self-frequency shifted optical solitons were observed in xenon [4], vibrational [8] and rotational [9] stimulated Raman scattering with low threshold was reported in hydrogen, highly efficient four-wave-mixing in air was demonstrated [10], and electromagnetically-induced transparency was observed with acetylene [11]. Self-channeling of subgigawatt femtosecond pulses hollow-core PBGFs was reported [12].

Generation of short pulses has always been of great scientific and technological interest. A well-known technique for compression of ultrashort pulses is based on the propagation dynamics of higher-order solitons in optical fibers [13]. When a pulse with sufficiently high peak power propagates in a medium with anomalous group velocity dispersion, dispersive effects can balance the effects of self-phase modulation and a fundamental soliton is formed. At sufficiently high input powers, higher-order solitons are formed resulting in oscillatory evolution of the temporal shape and spectrum of the pulse [13]. At the beginning of each period, the pulse undergoes significant compression [14] which depends on the soliton order. With appropriate

choice of fiber length, the output pulse can be significantly shorter than that at the input [14]. Since the wings of the pulse are not as well compressed as the central part, the compressed output pulse lies on a broad pedestal, which is a small fraction of the total energy [13]. The effects of higher-order dispersion [e.g. third-order dispersion (TOD)] and other nonlinearities (e.g. Raman scattering) become important when using femtosecond pulses, and although the periodic pulse evolution no longer occurs, temporal narrowing still takes place. Intrapulse Raman scattering shifts the soliton portion of the pulse envelope towards longer wavelengths and temporally separates it from the dispersive wave which results in pedestal-free short pulses [15]. TOD leads to oscillatory structure at the back end of the pulse and significantly degrades the optimal compression ratio [16]. It was shown [19] that the combination of negative TOD and intrapulse Raman scattering results in an increase in both the optimal compression ratio and in the peak power of the compressed pulses.

Another approach used for generating of short pulses involves a waveguide with normal dispersion followed by a dispersive delay line [20]. The nonlinear process of SPM in the waveguide broadens the pulse spectrum and, the dispersive delay line provides anomalous dispersion and compresses the pulse. Hollow-core waveguides filled with noble gases [21] are used for compression of femtosecond pulses with energies in the range of 50  $\mu\text{J}$  to 500  $\mu\text{J}$ , and compression of 400 nJ femtosecond pulses has been demonstrated with large-mode-area microstructured fibers [22].

Soliton compression in single-mode silica fibers is limited by the material damage threshold to pulse energies of a few nJ. The large diameter of the hollow capillaries used for pulse compression restricts the application of this technique to greater than 50 microjoule pulse energies. Here, we propose to use a hollow-core PBGF for soliton compression of pulses with energies in the region (10 nJ to 500 nJ) which bridges the gap between the other two techniques. In comparison with the hollow capillary scheme, PBGF provides the necessary anomalous dispersion for self-compression and there is no need to use a grating (prism) dispersive delay line.

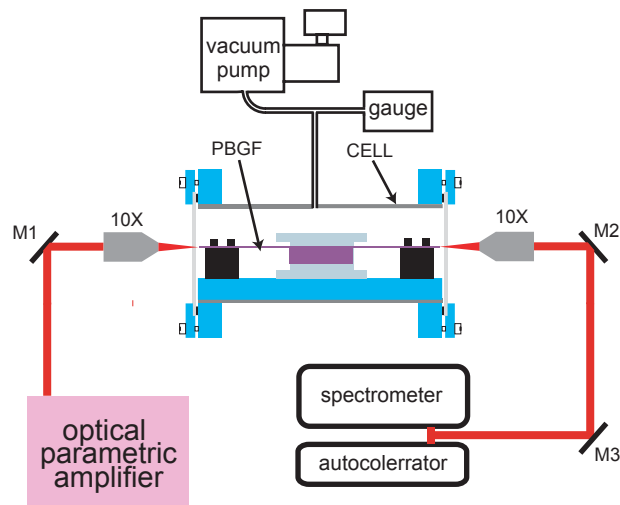


Fig. 1. The experimental setup.

In this paper, we report on soliton compression by more than a factor of two of megawatt pulses in Xe-filled PBGF. High fidelity pulses with widths of 50 fs and energies of 225 nJ were measured. The inherent large third-order dispersion of PBGFs degrades the optimal compression ratio. Our numerical simulations indicate that with these fibers, picosecond input pulses

can be compressed to less than 100 fs and thus allows for the possibility for soliton compression of pulses in 10nJ - 500 nJ regime.

## 2. Experiment

The experimental set-up is shown on Fig. 1. A regenerative amplification system (Hurricane, Spectra Physics) seeded by a Ti-sapphire oscillator pumps an optical parametric amplifier (OPA) that produces 100-fs pulses which are tunable in the range from 1100 to 1600 nm. We place a 24-cm-long piece of a Corning PBGF [2] inside a cell, which is evacuated for a few hours and then filled with Xe to a pressure of 4.5 atm. The input beam was coupled into the fiber with 10X aspheric objective (NewFocus), and the coupling efficiency is about 50%. The input pulses centered at 1470 nm are nearly transform limited (time-bandwidth product of 0.47, assuming a gaussian shape).

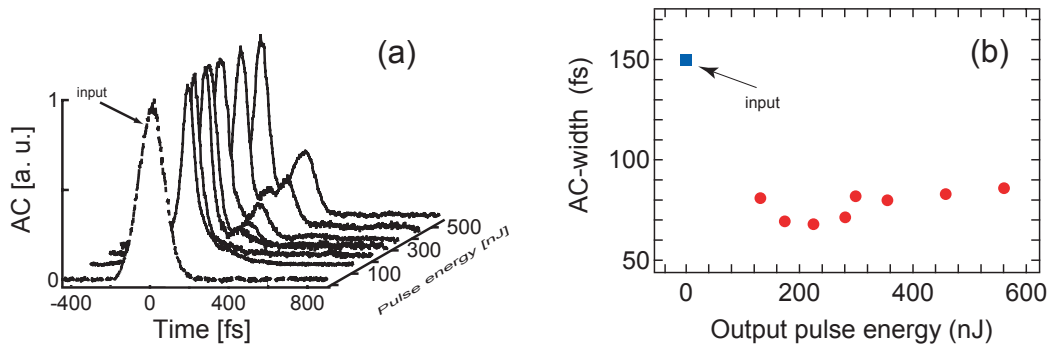


Fig. 2. (a) Measured autocorrelation traces as functions of pulse energy for a gas pressure of 4.5 atm, and (b) the autocorrelation width as a function of pulse energy.

The output pulse duration and spectrum are measured as functions of pulse energy. In Fig. 2 we plot a sequence of intensity autocorrelation traces for different pulse energies where the first trace is the autocorrelation trace of the input pulse. The narrowing of the autocorrelation trace indicates that the pulse undergoes temporal compression. For an energy of 225 nJ, the pulse width is half that of the input pulse (see Fig. 3a). The corresponding output spectrum is shown in Fig. 3b. We repeated the same measurements at a pressure of 9 atm and measured slightly greater compression (Fig. 3c and Fig. 3d). The observation of short-wavelength features slightly outside the transmission gap of the fiber is due to the fact that we are using a relatively short length of the fiber in our experiment, and thus frequency components outside the gap are not completely attenuated. As the pulse energy is increased, additional sidelobes in the autocorrelation trace are observed, which indicate the occurrence of pulse splitting associated with higher-order soliton formation.

## 3. Theory

We model pulse propagation inside the fiber using the one-dimensional nonlinear envelope equation with the inclusion of higher order dispersion and nonlinear terms. For the normalized amplitude  $u(z,t) = A(z,t)/A_0$ , where  $A(z,t)$  is the electric-field envelope and  $A_0$  is the peak amplitude of the input pulse, the propagation equation can be written as [23]

$$\frac{\partial u}{\partial \xi} = \sum_{n=2}^4 -(i)^{n-1} \frac{L_{ds}}{n! L_{ds}^{(n)}} \frac{\partial^n u}{\partial \tau^n} + i \left( 1 + \frac{i}{\omega_0 \tau_p} \frac{\partial}{\partial \tau} \right) P^{nl}, \quad (1)$$

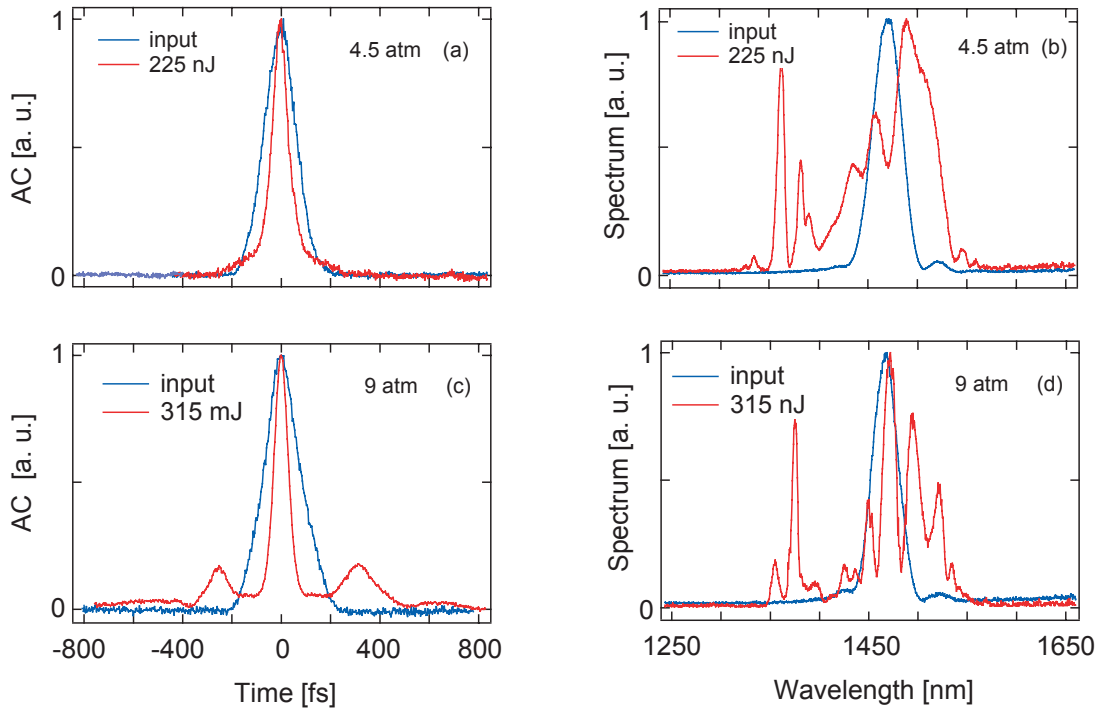


Fig. 3. Input (blue line) and output (red line) autocorrelation traces (a) and (c), and spectra (b) and (d) for a pulse energy of 225 nJ at gas pressure of 4.5 atm and for a pulse energy of 315 nJ at 9 atm, respectively.

where  $\tau = (t - z/v_g)/\tau_p$  is the retarded frame time normalized to the input pulse width ( $\tau_p$ ),  $\omega_0$  is the central frequency,  $L_{ds}^{(n)} = \tau_p^n/\beta_n$  is the  $n^{\text{th}}$ -order dispersion length,  $L_{ds}$  is the dispersion length, and  $\xi = z/L_{ds}$  is the normalized distance. In our simulations we include dispersion constants ( $\beta_n$ ) up to the fourth order. The values,  $\beta_2 = -182 \text{ fs}^2/\text{cm}$ ,  $\beta_3 = 5000 \text{ fs}^3/\text{cm}$ ,  $\beta_4 = 12000 \text{ fs}^4/\text{cm}$  are taken from our previous experimental data [4]. In general, the nonlinear polarization  $p^{nl}$  includes both instantaneous and non-instantaneous (i. e. Raman) contributions. Recent studies of the nonlinear properties of this fiber [5] show that the effective fiber nonlinearity is primarily due to the Xe gas ( $n_2 = 8.1 \times 10^{-19} \text{ cm}^2/\text{W}$  [24]), resulting in the absence of a Raman contribution to the nonlinear refractive index. Calculated spectra and autocorrelation for pulses with energies of 225 nJ and at a pressure of 4.5 atm are shown in Fig. 4. We see good agreement between the measured and calculated autocorrelations. Note that the calculated spectrum does not match well the measured one. We believe this is due to the fact that in our simulations we did not model the existence of the band gap and the calculated spectrum has features that are well outside the transmission window.

To underline the detrimental effect of third-order dispersion on the compression ratio, we compare in Fig. 5 the calculated output pulse intensity for the real case and when the third-order dispersion is neglected. Third-order dispersion leads to oscillatory structure at the pulse tail and splits the main peak in two. From these simulations, we believe that in our experiments, the broader central peak of the autocorrelation is a result of this oscillatory structure.

Nevertheless, we expect that by using pulses in the picosecond regime, far higher compression ratios should be possible. The severe effect of third-order dispersion is reduced, as seen from the ratio of the dispersion lengths in the nonlinear envelope equation,  $L_{ds}/L_{ds}^{(3)} =$

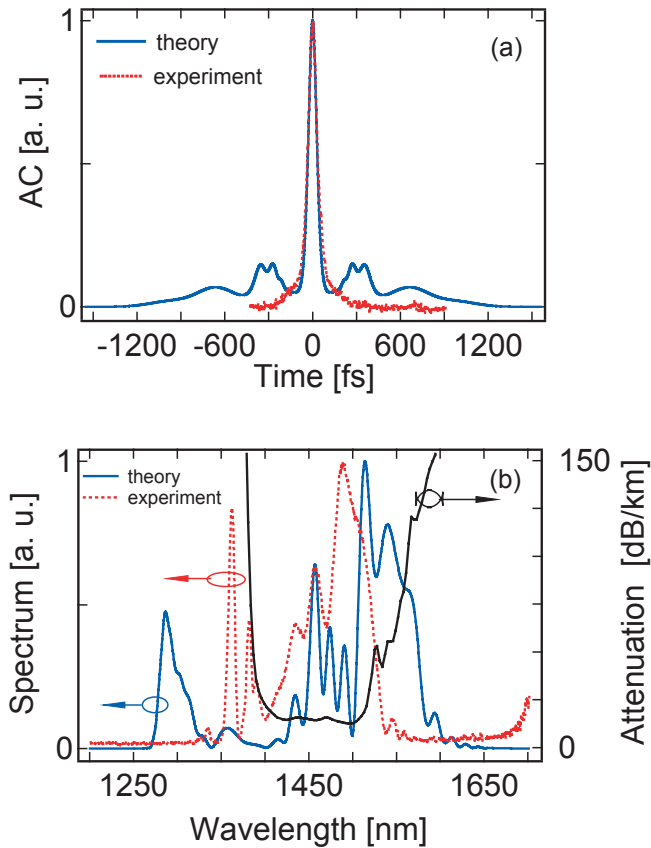


Fig. 4. Calculated (blue line) and measured (red line) autocorrelation (a) and spectrum (b) for a pulse with an energy of 225 nJ and for a gas pressure of 4.5 atm in the fiber. The black line in (b) is spectral attenuation of the fiber. The rise of the experimental spectrum at 1700 nm is a feature of the background level of the spectrometer.

$\beta_3/(\beta_2\tau_p)$ , which depends inversely on the pulse duration. Our simulations show that a pulse with an initial temporal duration of 1 ps and 20-nJ pulse energy can be compressed to 160 fs over 6 meters of this fiber at 4.5 atm gas pressure. If the input pulse energy is 210 nJ, 10th-order-soliton can be generated and compression down to 65 fs is expected (Fig. 6).

#### 4. Conclusion

In conclusion, we demonstrate soliton pulse compression of megawatt pulses in the 1500-nm regime in Xe-filled PBGF with high fidelity and with energies as high as 225 nJ. The large TOD of these fibers degrades the optimal compression ratio to a factor of 2.4 and further increases in the pulse energy leads to pulse splitting. In order to achieve higher compression ratios for femtosecond pulses, efforts need to be made to reduce the TOD in these fibers. However for picosecond input pulses, compression ratios greater than a factor of 10 can be achieved, and thus this scheme should enable compression of such pulses in 20-300 nJ regime.

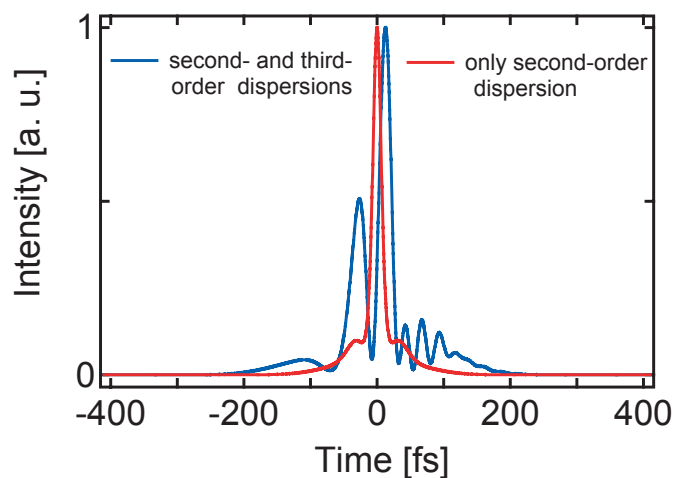


Fig. 5. Calculated output pulse intensity when only second-order dispersion is considered (red line) and when third-order dispersion is included (blue line).

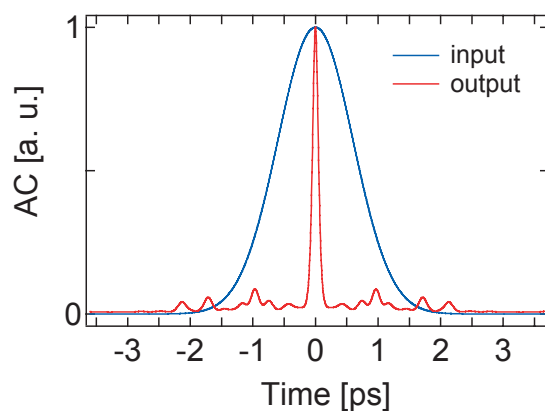


Fig. 6. Calculated autocorrelation for an input pulse (blue) with temporal duration of 1 ps and pulse energy of 210 nJ and the calculated output pulse autocorrelation (red) after propagation over 6 meters of this fiber.

### Acknowledgments

This work was supported by the Air Force Office of Scientific Research under contract number F49620-03-1-0223 and by the Center for Nanoscale Systems supported by NSF under award number EEC-0117770.